Secondary control for an Interconnected Power System using Model Predictive Control

Christof Goedhart (5055210), Soham Prajapati (5712297),

***Abstract*—In this paper a Model predictive control (MPC) strategy is designed to regulate the frequency in for a two-area power systems. MPC is a suitable choice for this task since it can take into account physical limitations of transmission lines like overheating and generation capacity. The MPC is designed for a discretized linear system of a two-area connected power system and it is formally shown that asymptotic stability is guaranteed. Numerical simulations are performed in MATLAB using the Casadi package.**

I. Introduction

A power system is said to be in balance when the power supplied by the generator and auxiliary systems are equal to the load demand from the consumers. At this point, the power system is said to be functioning at an equilibrium point, where the opposing electromagnetic and mechanical torque acting on the turbine shaft are equal in magnitude and thereby, the rotational speed of generator is constant. Suppose the load increases then there occurs an increase in the electromagnetic torque compared to mechanical torque supplied to the generator from the turbine. This decreases the generator rotor speed: decreasing the frequency of the system. Therefore, an imbalance of power in the power system can be directly referred to as the frequency deviation of the system. The control strategy employed to avoid this frequency deviation is called frequency control [1]. Today, many interconnected power systems use hierarchical control structure of three levels for frequency control: 1. primary control, 2. secondary control and 3. tertiary control [2]. The automatic activation of the available spinning reserve due to frequency changes, increasing the turbine input is referred to primary frequency control. This only ensures the stabilization of the system frequency as per the availability of the spinning reserve. To again achieve the frequency at scheduled value (frequency control) and maintain the net power interchanges with neighbouring control areas at their scheduled values (tie-line control) secondary control is required. In this work, secondary control is the area of focus for two-area interconnected power system.The tertiary control accounts for the econonomic energy dispatch which is not the scope of this work.

A simple proportional-integral (PI) controller is used as a standard secondary control, which are tuned based on the operator practice. However, the unpredictable nature of consumer activity and the advent of renewable energy penetration into the grid, makes the PI controller less suitable in terms of reliability [2] because of its key limitation to not handle the constraints. Ignoring the physical limitations of the system (constraints) could cause a reduction in lifetime of the components, thereby the entire power system. To overcome this and to provide optimal performance for frequency control, a Model Predictive Controller framework is employed in this work. For the sake of simplicity and understanding, we consider two-area interconnected power system as a case study.

Goedhart, C. and Prajapati, S. are master students at TU Delft, The Netherlands. E-mail addresses: {c.n.goedhart, s.r.prajapati}@student.tudelft.nl.

A. Paper Organization

The paper is structured as follows. In Section II, a linear continuous-time model is proposed, which is then discretized. In Section III, an MPC approach is formulated for the discrete linear system for two cases: state measurement MPC and output measurement MPC. In Section IV, proofs will be provided that show asymptotic stability of the closed-loop linearized system. In Section V, the performance of the closed-loop system system will be evaluated using simulations in MATLAB with Casadi package.

II. Discrete-time model

In this section, the dynamics of a seventh-order linear two-area connected power system is formulated on the basis of [3] and [4]. In a power system different power equipment with different voltage and power levels are connected together. However, the presence of various voltage and power levels causes problem in finding out the currents (or voltages) at different points in the network. To alleviate this problem, all the system quantities are converted into a uniform normalized platform. This is called the per unit system. In a per unit system each system variable or quantity is normalized with respect to its own base value. For ith area, Δf_i refers to the frequency deviation in Hertz (Hz), $\Delta P_{m,i}$ the per unit mechanical power change (pu), $\Delta P_{L,i}$ the per unit load change (pu), $\Delta P_{g,i}$ the governor valve position change (rad) and $\Delta P_{tie,ij}$ the per unit tie-line power change (pu) between ith and jth area. All these changes and deviation indicate the difference between actual and scheduled setpoints for the corresponding states. The output is measured as the area control error (ACE) as given in equation 2, where β_i is some constant bias factor. A negative ACE_i indicates that the area is generating less power than the desired power. Here it is used as an indicator of the load-generation power imbalance. Moreover, it is important to note that for an n-area connected system, there will be n-1 equations for $\Delta P_{tie,ij}$. For our system where $i = 1, 2$ the continuous system dynamics are given below.

$$\begin{cases} \Delta\dot{f}_i = \frac{1}{2H_i}(\Delta P_{m,i} - \Delta P_{L,i} - \Delta P_{tie,i}) - \frac{D_i}{2H_i}\Delta f_i \\ \Delta\dot{P}_{g,i} = \frac{1}{T_{g,i}}(\Delta P_{c,i} - \frac{1}{R_i}\Delta f_i - \Delta P_{g,i}) \\ \Delta\dot{P}_{m,i} = \frac{1}{T_{t,i}}(\Delta P_{g,i} - \Delta P_{m,i}) \\ \Delta\dot{P}tie_{12} = 2\pi(T_{12}\Delta f_1 - T_{12}\Delta f_2) \end{cases} . \tag{1}$$

$$ACE_i = \Delta P_{tie,i} + \beta_i \Delta f_i \tag{2}$$

As can be seen from the system of equations, the dynamics are linear. The system consists of seven states, $\mathbf{x} = [\Delta f_1, \Delta P_{g,1}, \Delta P_{m,1}, \Delta P_{tie,12}, \Delta f_2, \Delta P_{g,2}, \Delta P_{m,2}]^T$, two inputs as the control signal $\mathbf{u} = [\Delta P_{c,1}, \Delta P_{c,2}]^T$, and two disturbances $\mathbf{d} = [\Delta P_{L,1}, \Delta P_{L,2}]^T$. The following constants (from [3]) are provided: $H_1, H_2, D_1, D_2, R_1, R_2, T_{g,1}, T_{g,2}, \beta_1, \beta_2$. The system will have two outputs $\mathbf{y} = [ACE_1, ACE_2]^T$ The system, is discretized using zero-order hold (ZOH) with a sampling time of 0.1 seconds (equation 3) [5].

$$\begin{cases} x^+ = \Pi x + \Gamma u \\ y = Cx \end{cases} . \tag{3}$$

Where $\Pi = e^{Ah}$ and $\Gamma = \int_0^h e^{As} ds B$, A and B are state space matrices for continuous system and h is the sampling time. ZOH ensures that the discrete system is still controllable and observable. Moreover, it also balances the computation and communication burden of the system. The discretisation was done in MATLAB by using the c2d command, which takes the system equations and some sampling time and performs ZOH.

III. Model predictive control design

In this section, an MPC controller is designed to regulate the frequency of the two-area connected system considering the physical limitations of the components involved. This ensures that the system operation is safe. Assuming all the states are available for measurement, first, a full-state feedback MPC is designed for regulation of selected states. Next, considering only the output and adding disturbances to the system an output-feedback MPC is designed for regulation and disturbance rejection. Since, the MPC needs knowledge of the entire state-vector, a state estimator is also included for reconstructing the states.

A. Full-state feedback MPC

In this case, it is assumed that the system uses the information of all the states to determine the receding horizon MPC strategy with a control horizon of $N = 5$. The optimal control problem for online optimization is formulated below.

$$\mathbb{P}_N(x_0) : \begin{cases} \min\limits_{\mathbf{u_N}} & V_N(x_0, \mathbf{u_N}) \\ \text{s.t.} & \mathbf{u_N} \in \mathcal{U}_\mathcal{N}(x) \end{cases} \tag{4}$$

In 4, x_0 is the initial state at every iteration given as a parameter to the online optimization. The objective function with stage cost $l(\cdot)$ and terminal cost $V_f(\cdot)$ can be defined as,

$$V_N(x_0, \mathbf{u_N}) = \sum_{k=0}^{N-1} l(x(k), u(k)) + V_f(x(N)) \tag{5}$$

The stage cost penalizes the seven states and two inputs. The terminal cost penalizes the final state.

$$l(x(k), u(k)) = \frac{1}{2}(x(k)^T Q x(k) + u(k)^T R u(k)) \tag{6}$$

$$V_f(x(N)) = \frac{1}{2} x(N)^T P x(N) \tag{7}$$

where Q = $10I_{7\times7}$ and R = $1I_{2\times2}$ are tuned iteratively ensuring a balance between the control input, its rate of change and the settling time of states. The tuning procedure is explained in section V. The P is the solution to the discrete algebraic Riccati equation (DARE) used to solve the unconstrained infinite-horizon linear quadratic regulator (LQR) problem. This choice of P will help for stability proof discussed in section IV.

Moreover, in 4, $\mathcal{U}_\mathcal{N}$ represents the set of admissible control sequence for N steps such that the system solution $\phi(k; x, \mathbf{u_N})$ for $x(k+1) = \Pi x(k) + \Gamma u(k))$ and the inputs satisfy the constraints set $\mathbb{Z}$ and the terminal constraint $x(N) \in \mathbb{X}_f$.

Since in the system definition, the control input constraint set $\mathbb{U}$ and state constraint set $\mathbb{X}$ are independent ($\mathbb{U} \neq \mathbb{U}(x)$), $\mathbb{Z} = \mathbb{X} \times \mathbb{U}$. The state constraint set $\mathbb{X}$ consists of specific limits on two critical states: tie-line power change ($\Delta P_{tie,12}$) and governor valve position change ($\Delta P_{g,1}$ and $\Delta P_{g,2}$). The tie-line power deviation should be constrained to take into account the physical limitations of transmission lines due to overheating as tabulated in the work of [6]. It is very critical to account for the effects of overheating, because ignoring them could cause a total power blackout. Next major constraint to add is for the governor valve position change. The valve is constrained to open between -0.2 to 0.2 radians. For example, exceeding it more than 0.2 may cause a rapid drop in pressure of the steam generating boiler. Moreover, some margin of 0.3 is also kept over other state variables using system's knowledge. As a result, state constraint inequality $Fx(k) \leq e$ is formulated with F and e matrices as below.

$$\begin{bmatrix} I_{7\times7} \\ -I_{7\times7} \end{bmatrix} x(k) \leq \mathbf{1}_2 \otimes \begin{bmatrix} 0.3 \\ 0.2 \\ 0.3 \\ 0.03 \\ 0.3 \\ 0.2 \\ 0.2 \end{bmatrix} \tag{8}$$

In $\mathbb{Z}$, input constraint set $\mathbb{U}$ consists of two constraints. Note that the control input in the system are the actuation signal to the governor. This actuation signals usually have standard constraints [2] as given below.

$$\begin{bmatrix} I_2 \\ -I_2 \end{bmatrix} \begin{bmatrix} u_1(k) \\ u_2(k) \end{bmatrix} \leq \begin{bmatrix} 0.25 \\ 0.25 \\ 0.25 \\ 0.25 \end{bmatrix}$$
$$\implies Eu(k) \leq f \tag{9}$$

The terminal set $\mathbb{X}_f$ for the given system with constraint set $\mathbb{Z}$ has 48 closed inequalities of the form $Hx(N) \leq h$. The choice of this terminal set is discussed in section IV. In summary, for 4 following the notations of [7] the $\mathcal{U}_\mathcal{N}(x)$ can be given as

$$\mathcal{U}_\mathcal{N}(x) = \left\{ \mathbf{u_N} \;\middle|\; \begin{cases} \phi(k; x, \mathbf{u_N}) \in \mathbb{Z} & \forall k \in \mathbb{I}_{0:N-1} \\ \phi(k; x, \mathbf{u_N}) \in \mathbb{X}_f \end{cases} \right\} \tag{10}$$

So far, all the essential components of an MPC control framework have been defined for our problem. Now, it can be checked if our components allow an optimal solution for our framework. To check this, it is aimed to verify the existence of optimal solution using Proposition 2.4 in [7]. For our problem

- System dynamics in equation 1, stage-cost in equation 6 and terminal cost in equation 7 are continuous. Moreover, these three are zero at origin. Above two arguments satisfy assumption 2.2 in [7].
- It can be seen that all the constraints on inputs and states in $\mathbb{Z}$ are closed and bounded ($\leq$ inequalities and finite values). Using results from the work [8], since (1) (Π, C) is observable, (2) $\mathbb{X}$ is bounded, (3) $\lambda_i(\Pi) \leq 1$ (here $<$ 1) and (4) $\mathbf{0}_7 \in int(\mathbb{X})$, the terminal set $\mathbb{X}_f \subseteq \mathbb{X}$ is also compact. An alternative to above proof was used in this work to The terminal set was further confirmed to be bounded using `isbounded(polytope(H, h))` command using MPT3 Toolbox [9]. Moreover, each set contains origin. For origin in X_f, $H\mathbf{0}_7 - h < 0 \implies \mathbf{0}_7 \in int(\mathbb{X}_f)$. This allows the assumption 2.3 in [7] to hold.

Hence, from the fulfillment of above two assumptions, using Proposition 2.4 from [7] it can be said that there exists a set of initial conditions $x \in \mathcal{X}_N$ for which a solution exists for the optimal control problem $\mathbb{P}_N(x)$ in equation 4.

B. Output feedback MPC with Disturbance rejection

As seen from the above section, an MPC controller requires the full information of all the states in order to find the feasible solution online. In worst-case it should be able to confine attention to those states that can be steered to $\mathbb{X}_f$ in N steps (weak controllability [7]). In practice, for the system discussed here, not all the states are measurable. The current supervisory control and data acquisition systems usually involve measuring the area control error (ACE_i) at ith area which is linear combination of tie-line change $\Delta P_{tie,ij}$ and frequency deviation at ith area Δf_i. Moreover, the load acting at ith area $\Delta P_{L,i}$ is considered as a disturbance here because it is usually unknown. Therefore, to devise an MPC controller using output feedback, a Luenberger observer is used to reconstruct the states.

In order to deal with the disturbances, an augmented state-space system is used as shown below. The matrices Γ_d and C_d are added to model the effect of a constant disturbance $\Delta P_{L,i}$ on the system. The augmented state space system now has 9 states, it includes the 2 additional disturbances (one for each area in the power system).

$$\begin{bmatrix} x^+ \\ d^+ \end{bmatrix} = \begin{bmatrix} \Pi & \Gamma_d \\ 0 & I \end{bmatrix} \begin{bmatrix} x \\ d \end{bmatrix} + \begin{bmatrix} \Gamma \\ 0 \end{bmatrix} u$$
$$y = \begin{bmatrix} C & C_d \end{bmatrix} \begin{bmatrix} x \\ d \end{bmatrix} \tag{11}$$

Two additional requirements are that the original system needs to be observable and that equation 12 should hold. Which holds with $n + n_d$ = 9.

$$rank \begin{bmatrix} I - \Pi & -\Gamma_d \\ C & C_d \end{bmatrix} = n + n_d \tag{12}$$

For the disturbance rejection the optimal target selection (OTS) needs to be solved online (in each iteration), in order to determine the x_{ref} and u_{ref} such that $y_{ref} = 0$. The OTS optimization problem is defined below.

$$(x_{ref}, u_{ref})(\hat{d}, y_{ref}) \in \begin{cases} \text{argmin}_{x_r, u_r} J(x_r, u_r) \\ \text{s.t.} \begin{bmatrix} I - \Pi & -\Gamma_d \\ C & 0 \end{bmatrix} \begin{bmatrix} x_r \\ u_r \end{bmatrix} = \begin{bmatrix} \Gamma_d \hat{d} \\ y_{ref} - C_d \hat{d} \end{bmatrix} \\ (x_r, u_r) \in \mathbb{Z} \end{cases} \tag{13}$$

The Luenberger observer is defined in equation 14. The gain $L = \begin{bmatrix} L_1 \\ L_2 \end{bmatrix}$ was determined manually, such that $(\tilde{A} - L\tilde{C})$ is stable .

$$\begin{bmatrix} \hat{x}^+ \\ \hat{d}^+ \end{bmatrix} = \begin{bmatrix} \Pi & \Gamma_d \\ 0 & I \end{bmatrix} \begin{bmatrix} \hat{x} \\ \hat{d} \end{bmatrix} + \begin{bmatrix} \Gamma \\ 0 \end{bmatrix} u + \begin{bmatrix} L_1 \\ L_2 \end{bmatrix} (y - \begin{bmatrix} C & C_d \end{bmatrix} \begin{bmatrix} \hat{x} \\ \hat{d} \end{bmatrix}) \tag{14}$$

The cost function considered for output feedback MPC here is given below,

$$\begin{aligned} l(x(k), u(k)) &= (x(k) - x_{ref})^T Q (x(k) - x_{ref}) \\ &\quad + (u(k) - u_{ref})^T R (u(k) - u_{ref}) \\ V_f(x(N)) &= (x(N) - x_{ref})^T P (x(N) - x_{ref}) \end{aligned} \tag{15}$$

A high level overview of one iteration of the MPC framework here is the following. Initial conditions of the state and state-estimates are chosen such that they belong to $\mathcal{X}_N$ (discussed more in sections IV and V). The $\hat{d}$ is taken from vector $\hat{x}_0$ and given to the OTS. The OTS returns solution (x_{ref}, u_{ref}). The obtained values are given to the cost function from equation 15 which solves for input as the decision variables. The obtained input is used to further obtain the state and state estimate for the next instant using equations 11 and 14. The output and output estimates are obtained and state-estimate is used for $\hat{d}$ for the next iteration.

IV. Stability discussion - Asymptotic stability

It is relevant to note that, optimality does not imply stability, especially when the horizon is finite. The MPC controllers designed in above sections do regulation of states (in III-A) and output (in III-B). Since, both controllers try to achieve an equilibrium $(\bar{x}, \bar{u}) = (0, 0)$ it is required to analyse whether the equilibrium is asymptotically stable and is discussed in this

section using the methodology proposed in [7]. This methodology suggests to verify several assumptions to check if the optimal cost function V_N^0 is a valid candidate to be a Lyapunov function for our closed-loop system $x^+ = f(x, \kappa_N(x))$, where $\kappa_N(x)$ is the MPC control sequence determined in previous sections. If it does, then the origin is asymptotically stable for a set of initial conditions. The assumptions 2.2 and 2.3 are already verified to hold for our system as discussed at the end of section III-A. The system 3 with (Π, Γ) is controllable with controllability matrix $\mathcal{W}_n = [\Gamma \quad \Pi\Gamma \quad ...\Pi^5\Gamma]$ to be full rank. Before diving into other assumptions, a few choices made in the optimal control problem in equation 4 are discussed.

A. Choosing terminal cost V_f

The terminal cost in equation 7 is chosen to be the value function of infinite horizon unconstrainted optimal control problem, utilizing the solution P of the DARE equation. This choice is made so that the nominal stability can be inherited for at least some set of initial conditions (constraints do not allow choosing from $\mathbb{R}^7$) to obtain the solution for infinite horizon (but now) constrained optimal control problem. One more advantage here is that if the control horizon N is large enough, $x(N)$ will be in a neighbourhood of the origin where the optimal control law using LQR can take over and stabilize the system while respecting the state and input constraints. Moreover, this choice also makes the terminal cost a control Lyapunov function (CLF) which is further discussed in this section.

B. The choice of terminal set $\mathbb{X}_f$

The terminal set is a way to ensure recursive feasibility where we ensure that a feasible solution exists at each time step. For example, in regulation, we could either choose a strict constraint like $x(N) = 0$ or we can consider a non-conservative set in the vicinity of origin (containing the origin). It is more likely for the latter to attain a feasible solution because of the non-conservative form of the set. Keeping this idea in mind, we choose the largest set which satisfies the following,

- $\mathbb{X}_f$ satisfies the state and input constraints: $\mathbb{X}_f \subseteq \{x \in \mathbb{X} | Kx \in \mathbb{U}\}$.
- $\mathbb{X}_f$ is positive invariant: For $x \in \mathbb{X}_f$, $x^+ = Ax + Bu \in \mathbb{X}_f$ where $u = Kx$.

Generally, K for which $A+BK$ is stable is maximal constraint set. However, in order to ensure positive invariance, K needs to be the Riccati optimal gain [7]. So, an $\mathbb{X}_f$ satisfying above two conditions is known as maximal constraint admissible positive invariant set. This set was obtained in this work using `.LQRSet` command of MPT3 Toolbox. For our LTI system the resulting set can be defined as 48 linear inequalities of the form $Hx(N) \leq h$. This inequality was used as a constraint in the optimal control problem as given in equation 4.

In order to confirm that the above two conditions hold, MPC problem was solved and simulated with some initial conditions $x \in \mathbb{X}_f$ and ensuring that $f(x, \mathbf{u_N^0}) \in \mathbb{X}_f$. This also confirms the fact that state trajectory satisfied the set of state and input constraints in solving the problem.

C. The choice of $\mathcal{X}_N$

The set of initial conditions which give a feasible solution for the discussed optimal control problem is given by set $\mathcal{X}_N$. In the system considered, the number of states are 7. So, it will be difficult to visualize. However, to get a rough idea, the figure 1 illustrates the $\mathcal{X}_N$ for states Δf_1 and Δf_2. The other states are kept constant and at 0. The figure shows in green the initial conditions that can be steered to X_f, and in red those that cannot. 1600 combinations of f_1 and f_2 were evaluated, 40 for each. This same procedure can be repeated for the other states to get similar plots, and a more complete indication of $\mathcal{X}_N$.

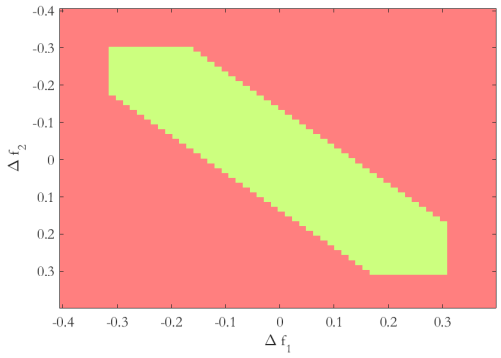

Fig. 1. 2-D mapping of $\mathcal{X}_N$ for states Δf_1 and Δf_2

D. Assumption 2.14

From above choice of $\mathbb{X}_f$, the positive invariant property can ensure that for all $x \in \mathbb{X}_f$ there exists u (such that $(x, u) \in \mathbb{Z}$) satisfies $f(x, u) \in \mathbb{X}_f$. Moreover, it can also be shown that the CLF here, $V_f(\cdot)$ satisfies for all $x \in X_f$,

$$V_f(x^+) - V_f(x) \leq -l(x, u) \tag{16}$$

From a posteriori simulations of the MPC framework for regulation, we plot the trajectory of it which in our case $V_f(x^+) - V_f(x) + l(x, u) \approx 0$ as seen in Figure 2. It is important to observe in this figure that the order of magnitude is 10^{-17} which is approximately zero.

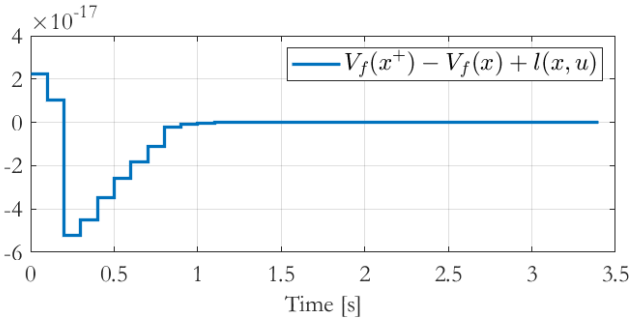

Fig. 2. Confirmation of $V_f(x)$ to be a Control Lyapunov Function. It can be seen that the order of magnitude is 10^{-17} which means $V_f(x^+) - V_f(x) + l(x, u) \approx 0$

The stage cost in equation 6 has $Q = 10I_{7\times7} > 0$ and $R = 1I_{7\times7} > 0$, which are hence positive definite. Therefore, $\forall x \in \mathcal{X}_N$ and $\forall u$ such that $(x, u) \in \mathbb{Z}$,

$$
\begin{aligned}
l(x,u) &= \frac{1}{2}(x(k)^T Q x(k) + u(k)^T R u(k) \\
&\geq \frac{1}{2}(x(k)^T Q x(k) \\
&\geq \alpha_1(|x|) \qquad (17)
\end{aligned}
$$

And from our choice of $V_f(x)$ from section IV-A, for $x \in \mathbb{X}_f$,

$$
\begin{aligned}
V_f(x) &= \frac{1}{2} x^T P x \\
&\leq \alpha_f(|x|) \qquad (18)
\end{aligned}
$$

In above results 17 and 18, $\alpha_1(\cdot)$ and $\alpha_f(\cdot)$ can be considered as $\mathcal{K}_\infty$ functions. Thus, from equations 16 , 17 and 18 the assumption 2.14 from [7] hold. Therefore, it is proven that the origin is asymptotically stable for our set of initial conditions in $\mathcal{X}_N$.

V. Numerical simulations

For regulation, the non-zero initial conditions given in the problem reflect the power imbalance in the system. The MPC should be able to steer all the states from this initial condition to the origin, thus steering the Δf for both the areas and ΔP_{tie} the power change connecting the areas by a tie-line to zero. Regulating these two states assure the regulation of the ACE for both the areas. A nominal settling time to assure good operation should be less than 10 seconds [3]. Thus, it is of utmost importance that the designed MPC framework is successful in regulating the area-control error for each area when starting from some non-zero initial conditions. In this section, we validate this using numerical simulations. The effects of different weighing matrices Q and R are first studied. Then we show the state-feedback regulation with the selected weights Q and R. Moreover, we test the controlled system with a disturbance in terms of constant load ΔP_{L1} added to both the areas to see if the controller is capable for disturbance rejection. To solve the optimal control problem from equation 4, we utilized `quadsol` solver from the open-source tool CasADi which uses a symbolic framework.

The initial conditions chosen in all the simulations such that x_0 outside $\mathbb{X}_f$ but within X_N. This was checked using the inequality for terminal set. The prediction horizon is set to N = 5.

A. Effects of weighing matrices Q and R

In this section, the effect of different cost function is shown. Since it is the relative values of the weighing that matters, we simulated the MPC for $Q = [0.1, 1, 10]$ keeping $R = 1$. Where Q is multiplied by an identity matrix which has the same dimension as the amount of states. The same goes for R which is multiplied by an identity matrix with the same dimension as the amount of inputs. As required the matrices Q and R are positive definite, since all values on the diagonal are positive. It was chosen to give all entries in the weighting matrices the same value since this was sufficient for regulation. Figure 3 shows the effect on the outputs, and figure 4 shows the effect on the inputs.

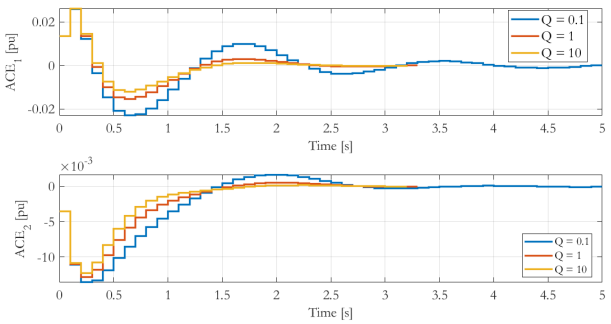

Fig. 3. Effect of weights on Output

In figure 3 it can be seen that that a lower Q (e.g. Q = 0.1) leads to more overshoot in both outputs than a higher Q (e.g. Q = 10). For a lower Q the 'penalty' on the states is relatively small compared to the 'penalty' on the inputs. This leads to slower convergence of the outputs to 0. In contrast, in figure 4 it can be seen that a lower Q leads to a quicker input convergence since it now has a 'higher priority'.

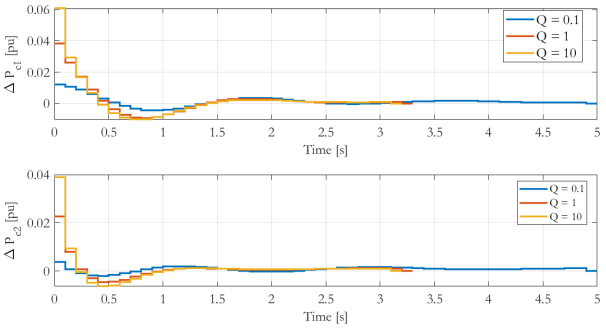

Fig. 4. Effect of weights on Input

B. Regulation using full-state feedback MPC

In figure 5 we see that the full state feedback MPC is able to accurately regulate the states. The settling time of Δf_1, $\Delta Ptie_{12}$ and Δf_2 is each around 2.5 seconds, with almost no overshoot.

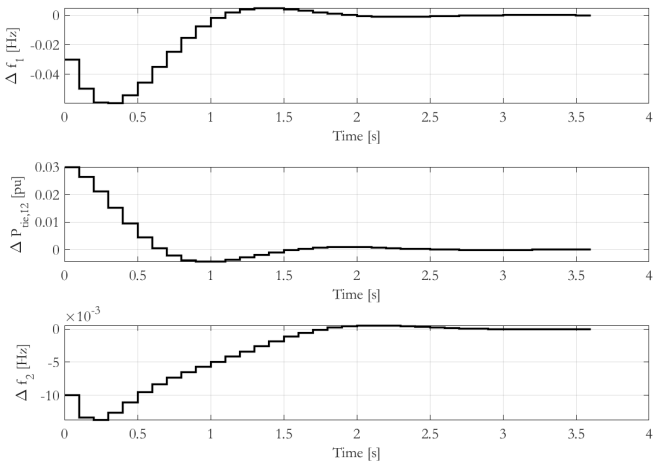

Fig. 5. Regulation of three states used as output

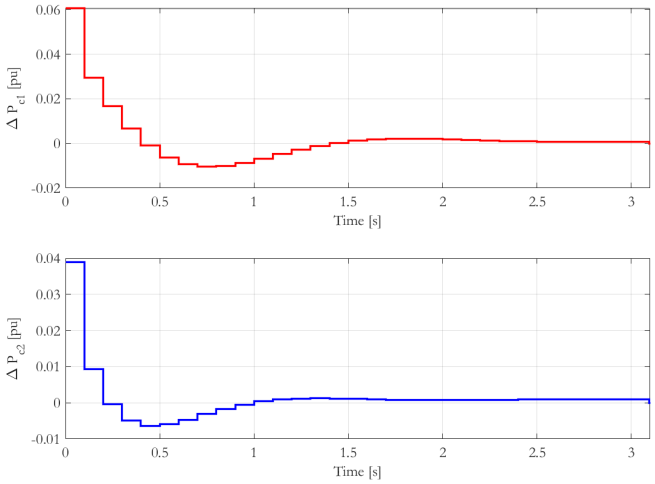

Fig. 7. Inputs trajectory: ΔP_{c1} and ΔP_{c2}

C. Regulation using output feedback MPC with disturbance rejection

For this simulation a constant disturbance was applied of 0.001. In the figure 6 it can be seen that the observer estimate quickly converges, indicating that the observer gains were well chosen. The ACE_1 and ACE_2 also quickly converge to 0, with little overshoot.

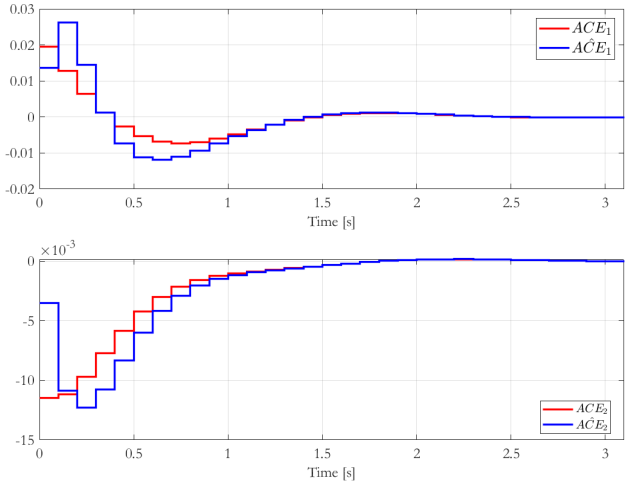

Fig. 6. Regulation of the outputs: ACE_1 and ACE_2 shown with observer estimate

When looking at figure 8 it can be seen that both estimates of the disturbances converge to the true disturbance of 0.001 in about 1.5 seconds.

D. Analysis and trouble-shooting after simulations

Near the end of our research process a discovery was made. It was noticed that the results of the designed MPC controller matched the results of an unconstrained LQR controller. This was unexpected since the initial conditions chosen in all the simulations were such that x_0 was outside of $\mathbb{X}_f$ but within

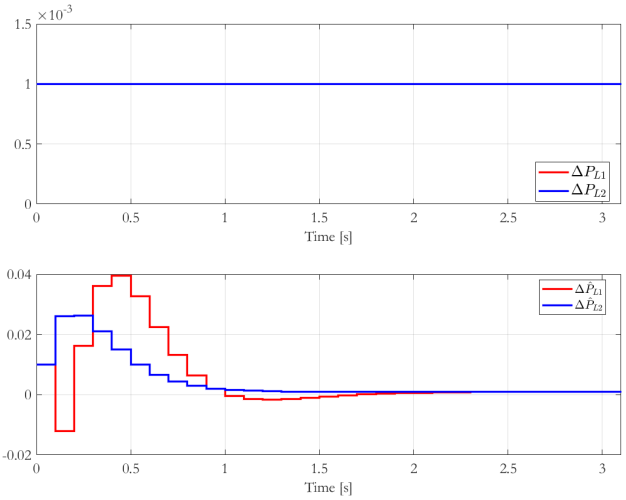

Fig. 8. Disturbance and its estimate. Note that disturbances are the constant loads added to the system at time 0

$\mathcal{X}_N$. So that the results should not be the same as LQR. Below, we list down some issues encountered and the actions taken to try resolving them.

- Choice of initial conditions: The initial conditions we choose are too close to origin keeping in mind the system undertaken and the constraints required. It is validated that the initial conditions are not in the terminal set by using $Hx_0 \leq h$. When the initial conditions are chosen from out of $\mathbb{X}$ the problem becomes infeasible and solver stops, despite the fact that all states were a function of the input: so the inputs should be capable to obtain a feasible solution. Even the constraints on inputs were removed to check if choosing the initial conditions out of $\mathbb{X}$ allow a feasible solution with control input as high as possible to bring all the states to get a feasible solution. Therefore, the constraints were once again reviewed but all looked correct. The state constraints were laid on $[x(1), x(2), ...x(N-1)]$ (without $x(0)$ since it is not a

function of input sequence) and terminal constraint as $Hx(N) \leq h$. However, the results were not positive and the solver returned infeasible solution error. It could also be that since the system constraints are close to origin, the system trajectory behave the same as an LQR. Moreover, the obtained set $\mathcal{X}_N$ as shown in figure 1 has bounds which are the same as the constraint set $\mathbb{X}$ for Δf_1 and Δf_2. This could also be one of the reasons.

- Choice of solver: In order to try a different route, the solver was changed from CasADI to YALMIP. The same framework was used in terms of the set of constraints on states and inputs. However, the same simulation results were obtained.

That being said, although the MPC controller does not provide an improved performance, it still gives the guarantee that all the provided input and state constraints are satisfied.

VI. Conclusion

While the task of designing a controller for an interconnected power system posed greater challenges than anticipated, it was observed that the physical constraints of these types of systems provide a good opportunity for MPC controllers to make a difference compared to traditional controllers. The numerical simulations didn't give the results that could be expected from a well-working MPC, it is suspected that somewhere in the implementation a small mistake is made. Still, insights can be gained from the system characteristics, stability analysis and different regulators that were designed.

References

[1] B. J. Machowski J, Lubosny Z and B. JR, *Power system dynamics stability and control*, ser. Third edition. John Wiley and Sons, 2020.

[2] A. M. Ersdal, I. M. Cecílio, D. Fabozzi, L. Imsland, and N. F. Thornhill, "Applying model predictive control to power system frequency control," pp. 1–5, 2013.

[3] H. Bevrani, *Robust power system frequency control*. Springer, 2014.

[4] A.-T. Tran, B. L. N. Minh, V. V. Huynh, P. T. Tran, E. N. Amaefule, V.-D. Phan, and T. M. Nguyen, "Load frequency regulator in interconnected power system using second-order sliding mode control combined with state estimator," *Energies*, vol. 14, no. 4, 2021. [Online]. Available: https://www.mdpi.com/1996-1073/14/4/863

[5] X.-C. Shangguan, Y. He, C.-K. Zhang, L. Jiang, and M. Wu, "Load frequency control of time-delayed power system based on event-triggered communication scheme," *Applied Energy*, vol. 308, 2022.

[6] A. M. Ersdal, D. Fabozzi, L. Imsland, and N. F. Thornhill, "Model predictive control for power system frequency control taking into account imbalance uncertainty," *IFAC Proceedings Volumes*, vol. 47, no. 3, pp. 981–986, 2014, 19th IFAC World Congress. [Online]. Available: https://www.sciencedirect.com/science/article/pii/S1474667016417428

[7] J. Rawlings and D. Mayne, *Model Predictive Control: Theory and Design*. Nob Hill Publishing, 2008.

[8] E. Gilbert and K. Tan, "Linear systems with state and control constraints: the theory and application of maximal output admissible sets," *IEEE Transactions on Automatic Control*, vol. 36, no. 9, pp. 1008–1020, 1991.

[9] M. Herceg, M. Kvasnica, C. N. Jones, and M. Morari, "Multi-parametric toolbox 3.0," in *2013 European control conference (ECC)*. IEEE, 2013, pp. 502–510.